doi:10.1093/plphys/kiab224 PLANT PHYSIOLOGY 2021: 186: 2051–2063

Plant Physiology®

Research Article

The histone variant H3.3 promotes the active chromatin state to repress flowering in Arabidopsis

Fengyue Zhao,[1,2] Huairen Zhang,[1] Ting Zhao ,[1] Zicong Li[3] and Danhua Jiang [1,2,*,†]

1 State Key Laboratory of Plant Genomics, Institute of Genetics and Developmental Biology, The Innovative Academy for Seed Design, Chinese Academy of Sciences, Beijing, 100101, China
2 University of Chinese Academy ofSciences, Beijing, 100039, China
3 School of Life Sciences, Shandong University, Qingdao, 266237, China

*Author for communication: dhjiang@genetics.ac.cn
†Senior author.

D.J. conceived the research. F.Z., T.Z., and D.J. performed the experiments. F.Z., H.Z., and D.J. analyzed the data. Z.L. provided the experimental materials. D.J. wrote the paper.
The author responsible for distribution of materials integral to the findings presented in this article in accordance with the policy described in the Instructions for Authors (https://academic.oup.com/plphys/pages/general-instructions) is: Danhua Jiang (dhjiang@genetics.ac.cn).

Abstract

The histone H3 family in animals and plants includes replicative H3 and nonreplicative H3.3 variants. H3.3 preferentially associates with active transcription, yet its function in development and transcription regulation remains elusive. The floral transition in Arabidopsis (*Arabidopsis thaliana*) involves complex chromatin regulation at a central flowering repressor *FLOWERING LOCUS C* (*FLC*). Here, we show that H3.3 upregulates *FLC* expression and promotes active histone modifications histone H3 lysine 4 trimethylation (H3K4me3) and histone H3 lysine 36 trimethylation (H3K36me3) at the *FLC* locus. The *FLC* activator FRIGIDA (FRI) directly mediates H3.3 enrichment at *FLC*, leading to chromatin conformation changes and further induction of active histone modifications at *FLC*. Moreover, the antagonistic H3.3 and H2A.Z act in concert to activate *FLC* expression, likely by forming unstable nucleosomes ideal for transcription processing. We also show that H3.3 knockdown leads to H3K4me3 reduction at a subset of particularly short genes, suggesting the general role of H3.3 in promoting H3K4me3. The finding that H3.3 stably accumulates at *FLC* in the absence of H3K36me3 indicates that the H3.3 deposition may serve as a prerequisite for active histone modifications. Our results reveal the important function of H3.3 in mediating the active chromatin state for flowering repression.

Introduction

Histone variants are related but functional distinct proteins in the same histone family (Talbert and Henikoff, 2017). The incorporation of histone variants could generate profound impacts on nucleosome property and chromatin function (Jiang and Berger, 2017; Talbert and Henikoff, 2017; Borg et al., 2021). The histone H3 family consists of three major variants: canonical H3.1/H3.2, H3.3, and CenH3/CENP-A (Hake and Allis, 2006; Jiang and Berger, 2017). Though H3.1 and H3.3 are distinguished by only a few amino acids, they acquired distinct expression patterns and deposition modes. The S phase-specific H3.1 is deposited during DNA replication via histone chaperone complex CHROMATIN ASSEMBLY FACTOR-1 (CAF1; Smith and Stillman, 1989), while H3.3 is expressed throughout the cell cycle and replication-independently incorporated into the chromatin by HISTONE REGULATORY HOMOLOG A (HIRA) complex,

Received April 9, 2021. Accepted April 29, 2021. Advance access publication May 10, 2021

ALPHA THALASSEMIA MENTAL RETARDATION SYNDROME X-LINKED (ATRX)-DAXX and DEK-domain containing protein (DEK; Tagami et al., 2004; Goldberg et al., 2010; Sawatsubashi et al., 2010; Talbert and Henikoff, 2017). Another histone chaperone ANTI-SILENCING FUNCTION 1 (ASF1) cooperates with both CAF1 and HIRA in the H3.1 and H3.3 deposition (Tagami et al., 2004). Although H3.1 plays an essential role in the chromatin assembly of doubled genome during DNA replication, the function of H3.3 is complex and remains undetermined. In both animals and plants, the lack of H3.3 causes defects in development (Hodl and Basler, 2009; Sakai et al., 2009; Szenker et al., 2012; Jang et al., 2015; Wollmann et al., 2017), demonstrating its important role in multicellular eukaryotes.

On the genome, H3.3 is associated with actively transcribed genes and gene regulatory elements (Wirbelauer et al., 2005; Goldberg et al., 2010; Szenker et al., 2011; Stroud et al., 2012; Wollmann et al., 2012). However, H3.3 is nonessential for most of the transcriptional events in *Drosophila* (*Drosophila melanogaster*; Hodl and Basler, 2009) and it is largely interchangeable with the replicative H3 (Sakai et al., 2009). In Arabidopsis (*Arabidopsis thaliana*), only a small number of H3.3-enriched genes show transcriptional defects when H3.3 levels are reduced, indicating that H3.3 may not be directly required for transcription (Wollmann et al., 2017). Other studies using different organisms and materials have shown that H3.3 modulates both active and repressive histone modifications (Banaszynski et al., 2013; Wollmann et al., 2017; Martire et al., 2019; Armache et al., 2020), adding to the complexity of the H3.3 function. Therefore, the role of H3.3 on transcription and chromatin modifications remains to be clarified. Besides its potential regulatory roles in histone modifications, H3.3 actively interplays with another histone variant H2A.Z. H2A.Z is associated with both gene activation and repression, likely depending on its genic localization and the chromatin context (Raisner et al., 2005; Jarillo and Pineiro, 2015; Chang et al., 2020). The coexistence of H3.3 and H2A.Z destabilizes nucleosomes (Fan et al., 2002; Jin and Felsenfeld, 2007), and H3.3 globally prevents the accumulation of H2A.Z at the 3′ gene end in Arabidopsis (Wollmann et al., 2017). However, the interaction between H3.3 and H2A.Z in the context of transcription regulation remains to be investigated.

Arabidopsis floral transition involves complex regulations at the chromatin level, and many of them act on a key floral repressor *FLOWERING LOCUS C* (*FLC*; He, 2012; Bao et al., 2020). In addition to *FLC*, the Arabidopsis genome encodes five FLC homologs, FLOWERING LOCUS M (FLM)/MADS AFFECTING FLOWERING 1 (MAF1)–MAF5, which act together with FLC to repress the floral transition (Ratcliffe et al., 2003; Scortecci et al., 2003; Kim and Sung, 2010; Gu et al., 2013). *FLC* activation requires permissive histone modifications, such as H3K4me3 and H3K36me3 (Xu et al., 2008, 2020; Jiang et al., 2009). H3K4me3 at *FLC* and its homologs *MAF4* and *MAF5* is catalyzed by the evolutionarily conserved COMPASS-like complex, which includes WDR5a, ASH2R, RBL, and a histone methyltransferase (Miller et al., 2001; Jiang et al., 2009, 2011, 2018; Ding et al., 2012). EARLY FLOWERING IN SHORT DAYS (EFS)/SET DOMAIN GROUP 8 (SDG8) is a major methyltransferase catalyzing H3K36 di- and trimethylation in Arabidopsis. In *efs* mutant, H3K36me2 and H3K36me3 are reduced at genome-wide level including the *FLC*, *MAF4*, and *MAF5* loci (Xu et al., 2008). The chromatin remodeling complex SWR1 (SWR1-C), which mediates H2A.Z deposition, also activates the expression of *FLC*, *MAF4*, and *MAF5* (Noh and Amasino, 2003; Deal et al., 2007). The disruption of SWR1-C leads to reduced *FLC* transcripts (Deal et al., 2007), suggesting a positive role of H2A.Z in *FLC* expression.

The expression of *FLC* is highly elevated in late-flowering Arabidopsis winter annual accessions by a FRIGIDA (FRI) containing protein complex (FRI-C). FRI-C interacts with several chromatin modifiers including COMPASS-like and EFS, and enhances their binding at the *FLC* locus (Jiang et al., 2009; Ko et al., 2010; Choi et al., 2011; Li et al., 2018; Luo and He, 2020). Hence, active histone modifications at *FLC* are elevated by FRI-C, resulting in strong *FLC* induction and flowering inhibition. In addition to promoting active histone modifications, FRI-C stimulates the *FLC* 5′ to 3′ gene looping (Li et al., 2018). Active *FLC* transcription per se does not regulate gene loop formation (Li et al., 2018), indicating that other mechanisms are responsible for the *FLC* 5′ to 3′ gene looping.

The presence of multiple chromatin modifications and their vigorous interactions at *FLC* makes it a paradigm for the understanding of chromatin-based plant gene regulation (He, 2012). Here, we show that H3.3 stimulates the expression of *FLC* and its homologs and promotes the active histone modifications at their loci. FRI directly interacts with the H3.3 chaperone HIRA and elevates H3.3 deposition toward the *FLC* 3′ region. The enriched H3.3 facilitates *FLC* 3′ end interaction with the 5′ end, promoting active histone modifications around the transcription start site (TSS) of *FLC*. Moreover, though H3.3 antagonizes H2A.Z, both of them are essential for *FLC* activation, and the loss of either one compromises *FLC* expression. In addition to *FLC* and its homologs, H3.3 is required for H3K4me3 at a subset of especially short genes. Our findings reveal the important function of H3.3 in the regulation of the active chromatin state, which enhances *FLC* transcription and floral repression.

Results

H3.3 represses the floral transition in Arabidopsis

A previous study has shown that H3.3 knockdown (*h3.3kd*) led to defects in leaf development and fertility (Wollmann et al., 2017). To further elucidate the function of H3.3 in plant development, we examined the flowering behavior of *h3.3kd*. *h3.3kd* lines *h3.3kd-1* and *h3.3kd-3* flowered earlier than the wild-type (WT) Columbia (Col; Figure 1, A and B; Supplemental Figure S1A). In Arabidopsis, the floral transition is repressed by FLC and its homologs. An examination of their expression by reverse transcription quantitative po-

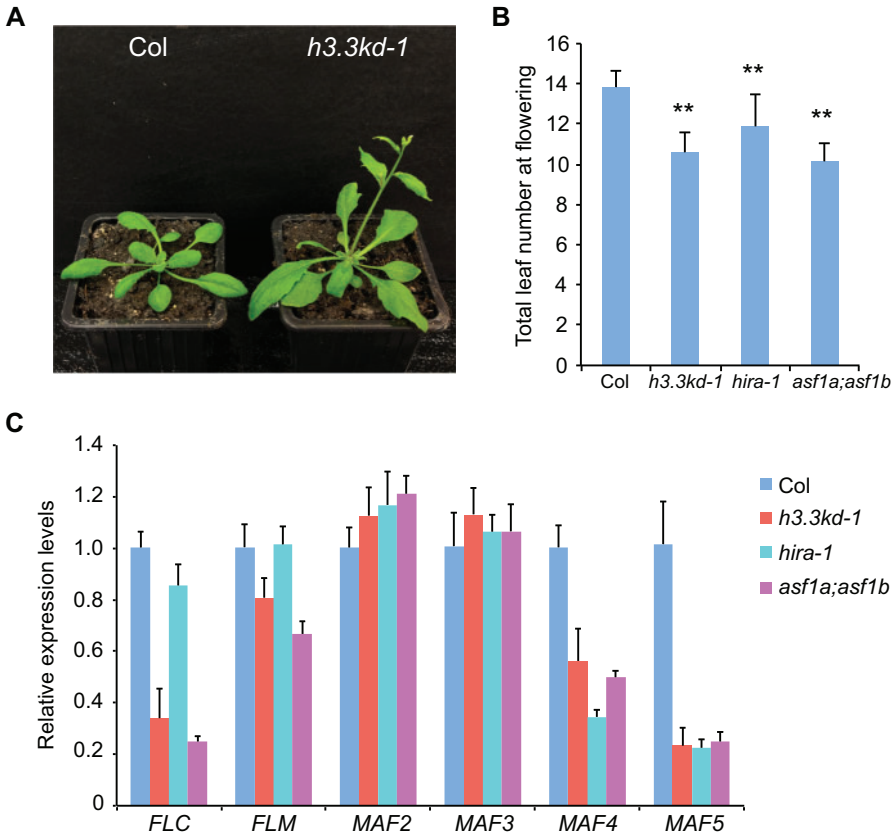

Figure 1 H3.3 represses flowering and activates the expression of *FLC* and its homologs. A, The flowering phenotype of *h3.3kd-1* grown in long days. B, The flowering time of indicated lines grown in long days. The total number of primary rosette and cauline leaves at flowering were counted; 15–20 plants were scored for each line. Values are means ± SD. Statistical significance relative to Col was determined by two-tailed Student's *t* test (**$P<0.01$). C, Relative transcripts of *FLC* and its homologs determined by RT-qPCR. *TUB2* was used as an endogenous control. Values are means ± SD of three biological repeats.

lymerase chain reaction (RT-qPCR) revealed that transcripts levels of *FLC*, *MAF4*, *MAF5* and to a lesser extent *FLM* were reduced in *h3.3kd* lines (Figure 1C; Supplemental Figure S1B; Wollmann et al., 2017), consistent with their early flowering phenotypes. H3.3 is deposited by the conserved HIRA complex (Nie et al., 2014; Duc et al., 2015). Moreover, two functional redundant ASF1 homologs ASF1a and ASF1b were identified in Arabidopsis (Zhu et al., 2011). Similar to *h3.3kd*, *hira* and *asf1a;asf1b* mutants showed early flowering phenotype and reduced expression of *FLC*, *MAF4*, and *MAF5* (Figure 1, B and C). The mild flowering phenotype and *FLC* reduction in *hira* mutant is likely due to the functional redundancy from other H3.3 deposition pathways mediated by ATRX or DEK (Sawatsubashi et al., 2010; Duc et al., 2017; Wang et al., 2018). As both *h3.3kd-1* and *h3.3kd-3* lines had similar flowering phenotypes and gene expression changes, we used *h3.3kd-1* for further analyses.

H3.3 promotes active histone modifications at *FLC* and its homologs

Previous RNA-seq results in *h3.3kd* have shown that only a small portion of H3.3-enriched genes were misregulated, suggesting that the loss of H3.3 per se might not be enough to alter transcription activity (Wollmann et al., 2017). The lack of H3.3 could reduce nucleosome density at the chromatin, which may affect transcription activity. We examined nucleosome enrichment at *FLC*, *MAF4*, and *MAF5* by profiling total H3 levels using chromatin immunoprecipitation (ChIP). The H3 levels were largely maintained with minimal reduction in *h3.3kd* (Figure 2, A and B; Supplemental Figure S2, A and B). It is possible that in *h3.3kd*, H3.1 compensates for the nucleosome deficit at *FLC*, *MAF4*, and *MAF5* loci.

We searched for other chromatin state changes that could contribute to gene expression defects induced by H3.3 knockdown. *FLC* activation requires active histone modifications including H3K4me3 and H3K36me3, both are highly enriched around the TSS of *FLC* (Yang et al., 2014; Li et al., 2016). We thus analyzed H3K4me3 and H3K36me3 levels at the *FLC* locus in *h3.3kd*. Considering the slight difference in H3 enrichment between WT and *h3.3kd*, histone modification levels were normalized to the H3 levels. H3K4me3 and H3K36me3 were reduced at *FLC* in *h3.3kd* (Figure 2, C and D), showing that H3.3 is required for their deposition at the *FLC* chromatin. Similarly H3K4me3 and H3K36me3 levels were significantly decreased at the TSS of *MAF4* and *MAF5* loci (Supplemental Figure S2, C and D). The *FLC* locus is also enriched with the repressive histone H3 lysine 27 trimethylation (H3K27me3; Jiang et al., 2008; Zhou et al., 2018). We

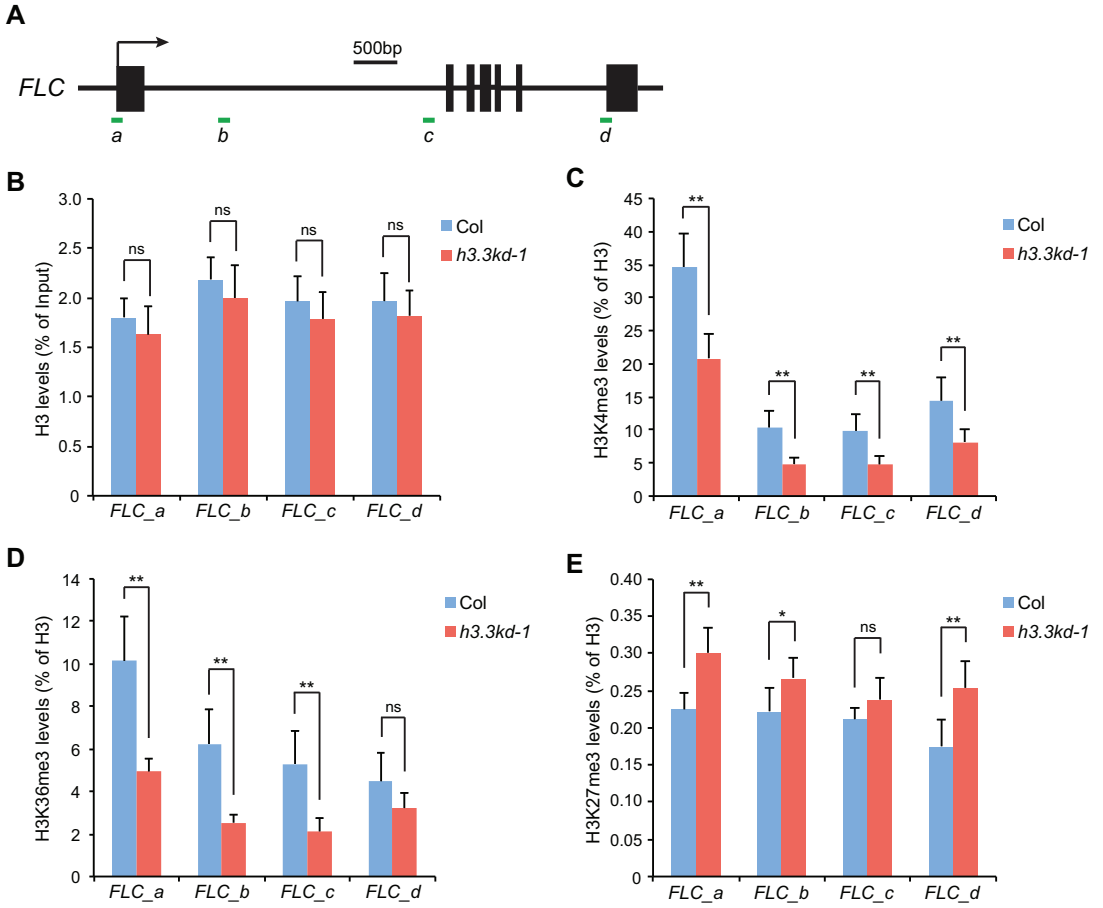

Figure 2 H3.3 promotes active histone modifications at *FLC*. A, Schematic structure of *FLC*. Filled boxes represent exons; an arrow indicates the transcription start site. ChIP examined regions are indicated by green lines. B–E, H3 (B), H3K4me3 (C), H3K36me3 (D), and H3K27me3 (E) levels at *FLC* determined by ChIP. The amounts of immunoprecipitated DNA fragments were quantified by qPCR and subsequently normalized to input DNA (B) or H3 antibody-precipitated DNA (C–E). Values are means ± SD of three biological repeats. Statistical significance was determined by two-tailed Student's *t* test (**$P<0.01$; *$P<0.05$; ns, not significant, $P>0.05$).

observed a moderate increase of H3K27me3 in *h3.3kd* compared to WT, especially at the *FLC* 5′ and 3′ gene ends (Figure 2E). This could be due to the antagonism between H3K27me3 and active histone modifications at *FLC* (Jiang et al., 2008; Yang et al., 2014), or the loss of H3.3-induced H3.1 accumulation, which closely associates with and facilitates methylation at H3K27 (Stroud et al., 2012; Jacob et al., 2014; Jiang and Berger, 2017). Together, these results suggest that H3.3 promotes active histone modifications at *FLC*, *MAF4*, and *MAF5*.

FRI-mediated *FLC* activation requires H3.3

In winter-annual Arabidopsis accessions, FRI elevates *FLC* expression to levels that inhibit flowering before winter (Johanson et al., 2000; Michaels et al., 2003). To evaluate the role of H3.3 in FRI-mediated *FLC* upregulation, we introduced a functional *FRI* allele into *h3.3kd* (Lee et al., 1994), and observed that *h3.3kd* strongly suppressed the late-flowering phenotype of *FRI* (Figure 3, A and B). The suppression of the late-flowering phenotype by *h3.3kd* is likely due to the reduction of *FLC* expression, hence, we examined its expression in *h3.3kd-1*;*FRI*. Indeed, elevated *FLC* expression levels in *FRI* were reduced upon H3.3 knockdown (Figure 3C). Autonomous pathway genes such as *FVE* and *FLOWERING LOCUS D* (*FLD*) repress *FLC* expression, the loss of *FVE* or *FLD* causes delayed flowering due to *FLC* upregulation (He et al., 2003; Ausin et al., 2004). We further crossed *h3.3kd* with *fve-4* and *fld-3* mutants; similarly the late flowering phenotypes and upregulated *FLC* transcripts of *fve-4* and *fld-3* were suppressed by *h3.3kd* (Supplemental Figure S3). Therefore, H3.3 is required for *FLC* activation induced by FRI and autonomous pathway mutations.

FRI acts in FRI-C, which recruits and stabilizes chromatin modifiers at the *FLC* locus, and thus promotes active histone modifications including H3K4me3 and H3K36me3 at *FLC* (Choi et al., 2011; Li et al., 2018). We found that FRI-induced H3K4me3 and H3K36me3 at *FLC* were strongly suppressed by *h3.3kd* (Figures 2A; 3, D and E). These results demonstrate that H3.3 is essential for FRI-mediated establishment of active histone modifications at *FLC*.

Enhanced H3.3 deposition mediated by FRI promotes *FLC* gene loop formation

To investigate whether FRI regulates H3.3 deposition at the *FLC* locus, we combined an *HTR5-GFP* (*HTR5* is one of the

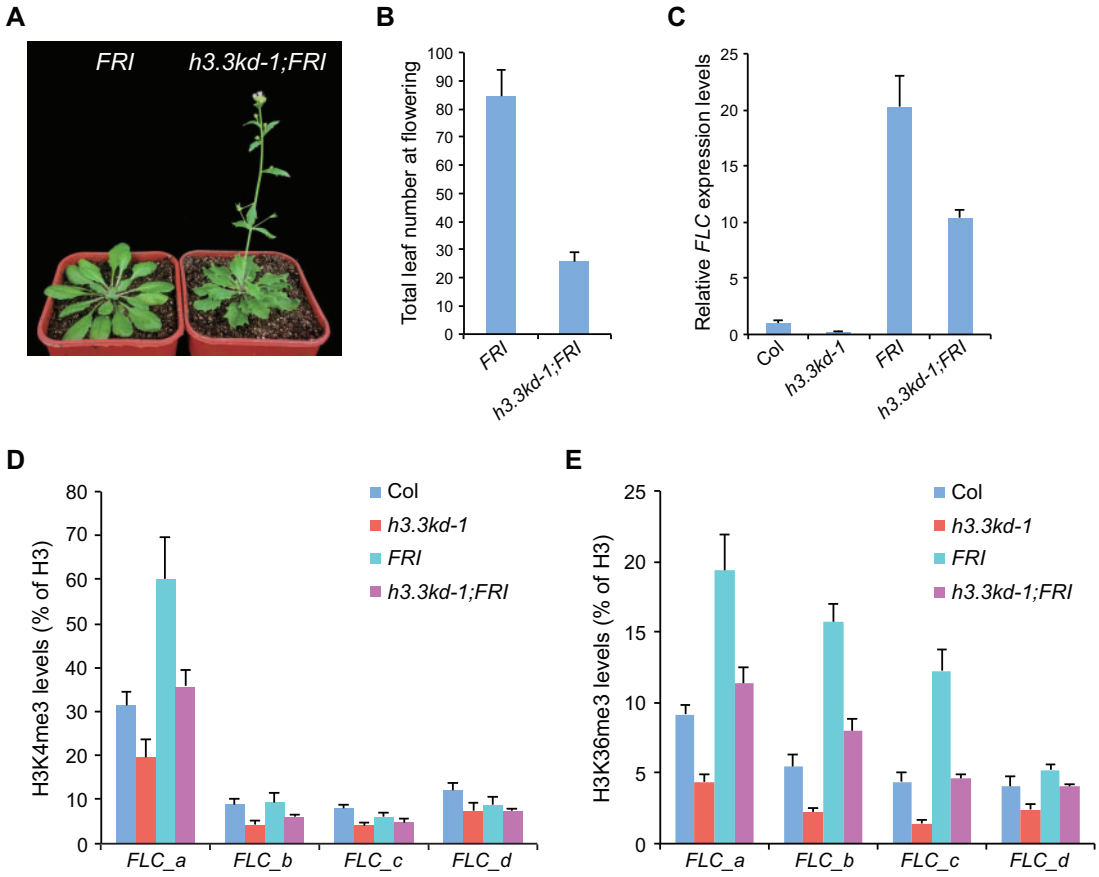

Figure 3 FRI-induced *FLC* upregulation and active histone modifications require H3.3. A, The flowering phenotype of *h3.3kd-1;FRI* grown in long days. B, The flowering time of indicated lines grown in long days. The total number of primary rosette and cauline leaves at flowering were counted; 10 and 16 plants were scored for *FRI* and *h3.3kd-1;FRI*, respectively. Values are means ± SD. C, Relative transcripts of *FLC* determined by RT-qPCR. *TUB2* was used as an endogenous control. Values are means ± SD of three biological repeats. D, E, H3K4me3 (D) and H3K36me3 (E) levels at *FLC* determined by ChIP. The amounts of immunoprecipitated DNA fragments were quantified by qPCR, and subsequently normalized to H3 antibody-precipitated DNA. Values are means ± SD of two biological repeats.

three H3.3 coding genes in Arabidopsis) reporter line with the functional *FRI* and performed ChIP experiment. Due to the lack of specific antibody against plant H3.3, the levels of HTR5-GFP at chromatin were used as an indication for H3.3 deposition levels (Wollmann et al., 2012). The enrichment of HTR5-GFP was enhanced by FRI especially toward the *FLC* 3′ region (Figures 2A, 4A), while the overall protein abundance of HTR5-GFP was not affected by FRI (Supplemental Figure S4A). Thus, FRI induces H3.3 deposition at the *FLC* chromatin.

To explore how FRI enriches H3.3 at *FLC*, we tested the interactions between FRI-C and the H3.3 chaperones. Direct interaction of FRI with HIRA was detected by pull-down assay (Figure 4B). Bimolecular fluorescence complementation (BiFC) experiment further confirmed that FRI directly associates with HIRA (Figure 4C). Moreover, co-immunoprecipitation (Co-IP) assay was performed with FRI-HA and HIRA-Myc coexpressed Arabidopsis protoplasts. HIRA-Myc was copurified with FRI-HA but not with the HA antibody-coupled beads (Figure 4D). Together, these results indicate that FRI-C directly enriches H3.3 deposition at *FLC* by interacting with its chaperone HIRA complex.

In plants, H3K4me3 and H3K36me3 are accumulated at the TSS of transcribed genes (Sequeira-Mendes et al., 2014; Liu et al., 2019). A similar pattern was observed at the *FLC* locus (Figure 2, A, C, and D; Yang et al., 2014; Li et al., 2016). However, H3.3 is generally enriched around the 3′ gene end (Stroud et al., 2012; Wollmann et al., 2012). Moreover, though FRI enhances H3K4me3 and H3K36me3 levels mainly around the *FLC* 5′ region, the elevated deposition of H3.3 mediated by FRI is more predominant toward the gene body and 3′ end (Figures 2A; 3, D and E; 4A). At the *FLC* locus, a peak of H3.3 was also detected at TSS (Figures 2A, 4A). The H3.3 enrichment at both gene ends is a signature chromatin state for moderately expressed genes with a gene loop structure (Liu et al., 2016). The 5′ and 3′ of *FLC* form a gene loop and this structure is enhanced by FRI (Crevillen et al., 2013; Li et al., 2018). We thus performed a chromosome conformation capture (3C) experiment to examine the impact of H3.3 on 5′ to 3′ looping. Interestingly, the loss of H3.3 impaired loop formation at *FLC* (Figure 4E). Thus, H3.3 facilitates *FLC* 5′ to 3′ loop formation (Figure 4F).

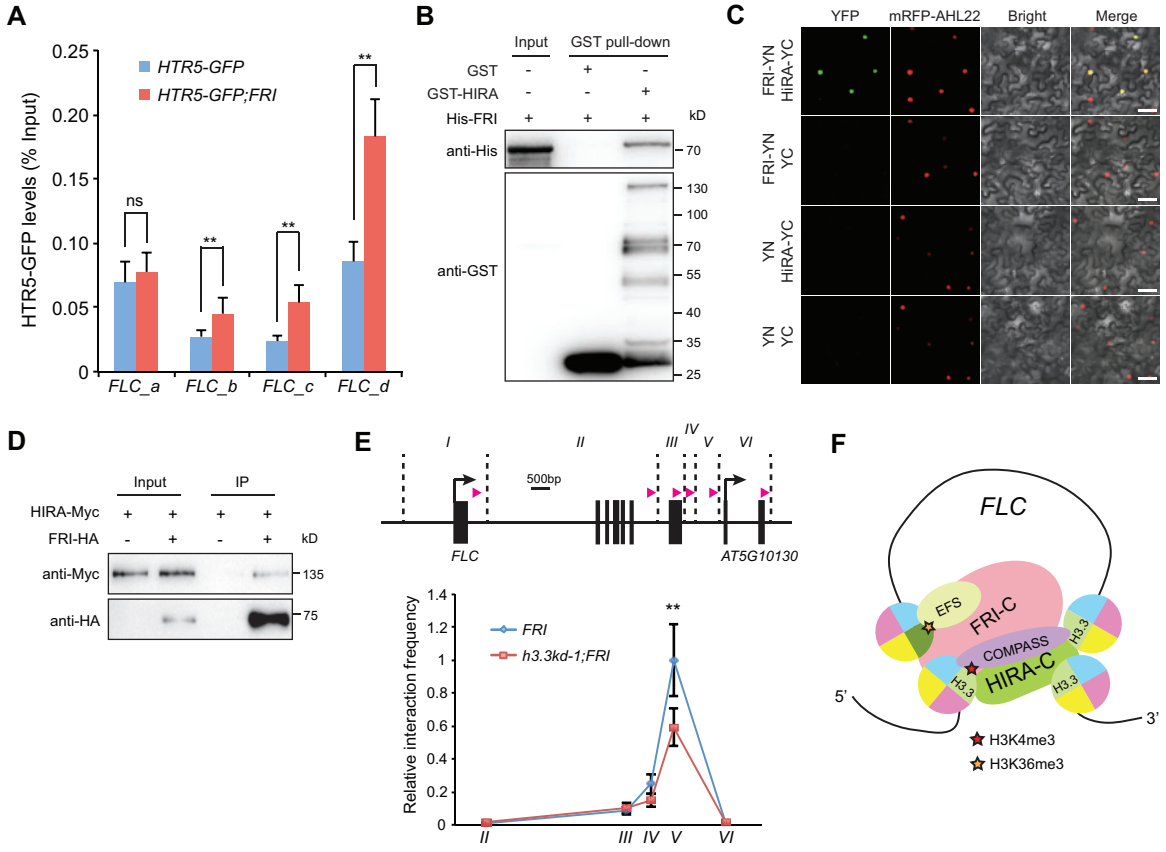

Figure 4 FRI-enriched H3.3 deposition promotes *FLC* 5′ to 3′ looping. A, HTR5-GFP enrichment levels at *FLC* in indicated lines. The amounts of immunoprecipitated DNA fragments were quantified by qPCR and normalized to input DNA. Values are means ± SD of three biological repeats. Statistical significance was determined by two-tailed Student's *t* test (**$P<0.01$; ns, $P>0.05$). B, Pull-down assay of glutathione S-transferase (GST)-HIRA with His-FRI. C, Physical interaction of FRI-NYFP (YN) with HIRA-CYFP (YC) in *N. benthamiana* leaf cells analyzed by BiFC. mRFP-fused AHL22 (AT-hook motif nuclear-localized protein 22) signals were used to label nuclei (Meng et al., 2019). Scale bars: 50 μm. D, Co-IP assay of HIRA with FRI. Total proteins were extracted from Arabidopsis protoplasts coexpressing HIRA-Myc and FRI-HA. E, Quantitative 3C of the *FLC* 5′ to 3′ loop formation using region I as the anchor region in indicated lines. In the up graph, *BamH*I and *Bgl*II cutting sites are indicated by the vertical dashed lines, pink arrow indicates the position and direction of the primer used in each region. The interaction frequency was normalized to that of region I to region V in *FRI*, which was set as 1.0. Values are means ± SD of three biological repeats. Statistical significance was determined by two-tailed Student's *t* test (**$P<0.01$). F, A possible function for H3.3 in FRI-induced active histone modifications and gene looping at *FLC*. FRI-C enhances the H3.3 deposition toward the *FLC* 3′ end. The enriched H3.3 may stabilize the binding of histone modifiers such as COMPASS-like at the spatially nearby 5′ and 3′ ends, and/or stimulate the activity of histone modifiers, resulting in increased gene loop formation and induced active histone modifications predominantly at the 5′ end.

H3.3 and H2A.Z are both required for *FLC* activation but oppose each other at the *FLC* chromatin

Activation of *FLC* and its homologs also depends on the chromatin remodeling complex SWR1-C that deposits H2A.Z. Disruption of SWR1-C led to downregulated *FLC*, *MAF4*, and *MAF5* expression and accelerated flowering (Noh and Amasino, 2003; Deal et al., 2007), presumably due to the lack of H2A.Z at their chromatin. To directly address the impact of H2A.Z on flowering gene expression, we used a near-null *h2a.z* mutant defective in all three H2A.Z coding genes, which similarly showed early flowering phenotype (Figure 5, A–C; Coleman-Derr and Zilberman, 2012). In addition to *FLC*, *MAF4*, and *MAF5*, the loss of H2A.Z led to the reduced expression of *FLM* and *MAF3* (Figure 5D). Thus, our results confirmed that H2A.Z activates *FLC* and its homologs.

We sought to investigate how H3.3 and H2A.Z, both of them required for the activation of *FLC*, interact at its loci. H2A.Z is enriched at both the 5′ and 3′ of *FLC* (Figures 2A, 5E), consistent with a similar pattern reported previously (Deal et al., 2007). Interestingly, H3.3 knockdown enhanced H2A.Z occupancy at *FLC* (Figure 5E), despite reduced *FLC* expression in *h3.3kd*. To examine H3.3 accumulation in the absence of H2A.Z, HTR5-GFP enrichment was quantified by ChIP-qPCR after it was introduced into *h2a.z* mutant. A slight induction of HTR5-GFP levels was detected toward the *FLC* 3′ end (Figures 2A, 5F). This is not due to the increased expression of HTR5-GFP, as its protein levels were rather decreased in *h2a.z* for unknown reasons (Supplemental Figure S4B). We also confirmed that *FLC* expression was reduced in *HTR5-GFP;h2a.z* (Supplemental

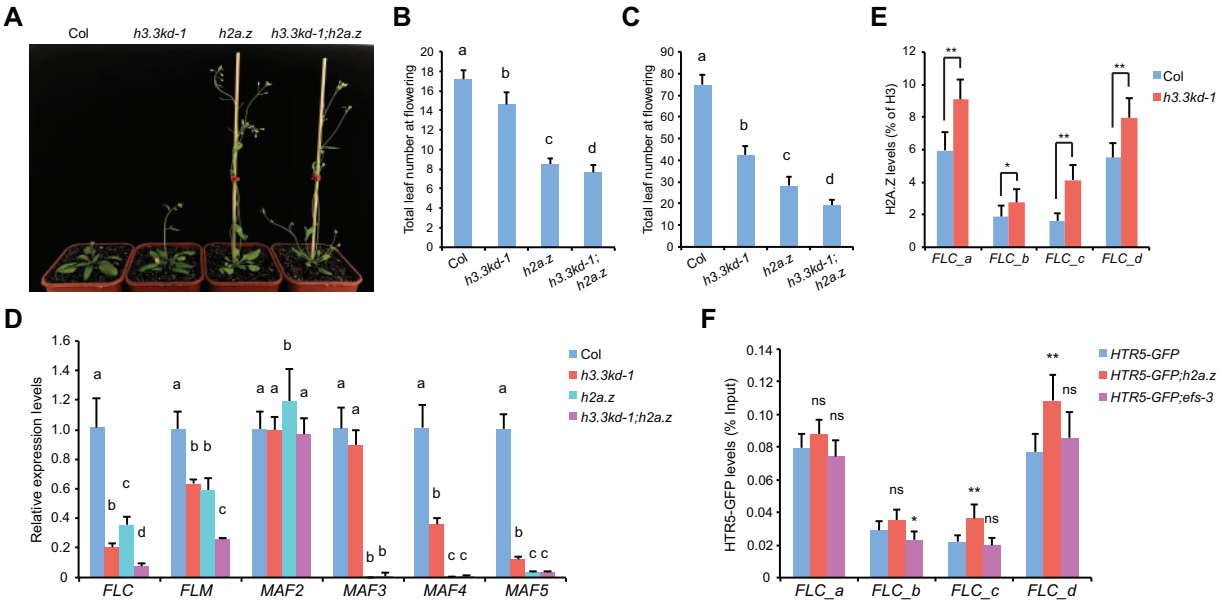

Figure 5 H3.3 and H2A.Z oppose each other at the *FLC* chromatin but coactivate *FLC* expression. A, The flowering phenotype of indicated lines grown in long days. B and C, The flowering time of indicated lines grown in long days (B) and short days (C). The total number of primary rosette and cauline leaves at flowering were counted. For (B), 15–18 plants were scored for each line. For (C) 9 plants were scored for each line. Values are means ± SD. The significance of differences was tested using one-way ANOVA with Tukey's test ($P<0.05$), different letters indicate statistical significance. D, Relative transcripts of *FLC* and its homologs determined by RT-qPCR. *TUB2* was used as an endogenous control. Values are means ± SD of three biological repeats. The significance of differences at each gene was tested using one-way ANOVA with Tukey's test ($P<0.05$), different letters indicate statistical significance. E, H2A.Z levels at *FLC* determined by ChIP. The amounts of immunoprecipitated DNA fragments were quantified by qPCR, and subsequently normalized to H3 antibody-precipitated DNA. Values are means ± SD of three biological repeats. Statistical significance was determined by two-tailed Student's *t* test (*$P<0.05$; **$P<0.01$). F, HTR5-GFP enrichment levels at *FLC* in indicated lines. The amounts of immunoprecipitated DNA fragments were quantified by qPCR and normalized to input DNA. Values are means ± SD of three biological repeats. Statistical significance relative to HTR5-GFP was determined by two-tailed Student's *t* test (*$P<0.05$; **$P<0.01$; ns, $P>0.05$).

Figure S4C). Thus, although both are activators of *FLC*, H3.3 and H2A.Z antagonize each other at the *FLC* locus.

We next tested the genetic relationship of H3.3 and H2A.Z in flowering by crossing *h3.3kd* with *h2a.z*. H3.3 knockdown in *h2a.z* further enhanced the reduction of especially *FLC* and *FLM* transcripts (Figure 5D), and concomitantly accelerated flowering in both long-day and short-day conditions (Figure 5, B and C). Together, these results suggest close cooperation of H3.3 and H2A.Z on *FLC* activation and the presence of both H3.3 and H2A.Z is required to maintain *FLC* at a transcription active state in Col, while lacking of either one (even when the enrichment of the other one is increased) leads to a reduction in *FLC* expression.

H3K36me3 is not required for H3.3 accumulation at *FLC*

The above results suggest that H3.3 regulates chromatin modifications at *FLC*. To investigate the impact of chromatin modifications on H3.3 deposition, we examined H3.3 enrichment with mutants defective in chromatin modifications. EFS deposits H3K36me3 at *FLC* to stimulate its expression. We measured HTR5-GFP accumulation at *FLC* in *efs* mutant, in which *FLC* expression is reduced (Supplemental Figure S4C). The HTR5-GFP protein expression levels and its enrichment at *FLC* were comparable to that in WT (Figure 5F; Supplemental Figure S4B), suggesting that H3K36me3 is not required for H3.3 deposition.

H3.3 knockdown affects H3K4me3 at a subset of loci

A previous study has shown that H3.3 knockdown had little impact on H3K4me3 globally when all the genes were evaluated, while H3K36me3 enrichment was affected especially at misexpressed genes upon the loss of H3.3 (Wollmann et al., 2017). To further investigate the impact of H3.3 at H3K4me3 in detail, we analyzed the published ChIP-seq data generated using *h3.3kd-3* seedlings to identify genes with altered H3K4me3 levels. ChIP-seq detected less H3K4me3 at *FLC*, *MAF4*, and *MAF5* in *h3.3kd-3*, confirming that H3.3 is required for H3K4me3 at these loci (Supplemental Figure S5A). The lack of H3.3 led to strong H3K4me3 reductions at 761 loci (>1.5-fold change), while 116 loci gained H3K4me3 in *h3.3kd* (Figure 6, A and B; Supplemental Table S1). In line with the role of H3K4me3 in gene activation, genes with reduced H3K4me3 showed lower expression levels in *h3.3kd* (Figure 6C). Notably, the H3K4me3 is broadly distributed at these genes, albeit it is generally enriched around the TSS (Figure 6B). Such a distribution pattern resembles H3K4me3 enrichment at genes with short length (Li et al., 2016). We thus examined the length of genes that displayed H3K4me3 reduction in *h3.3kd* and found that they were indeed

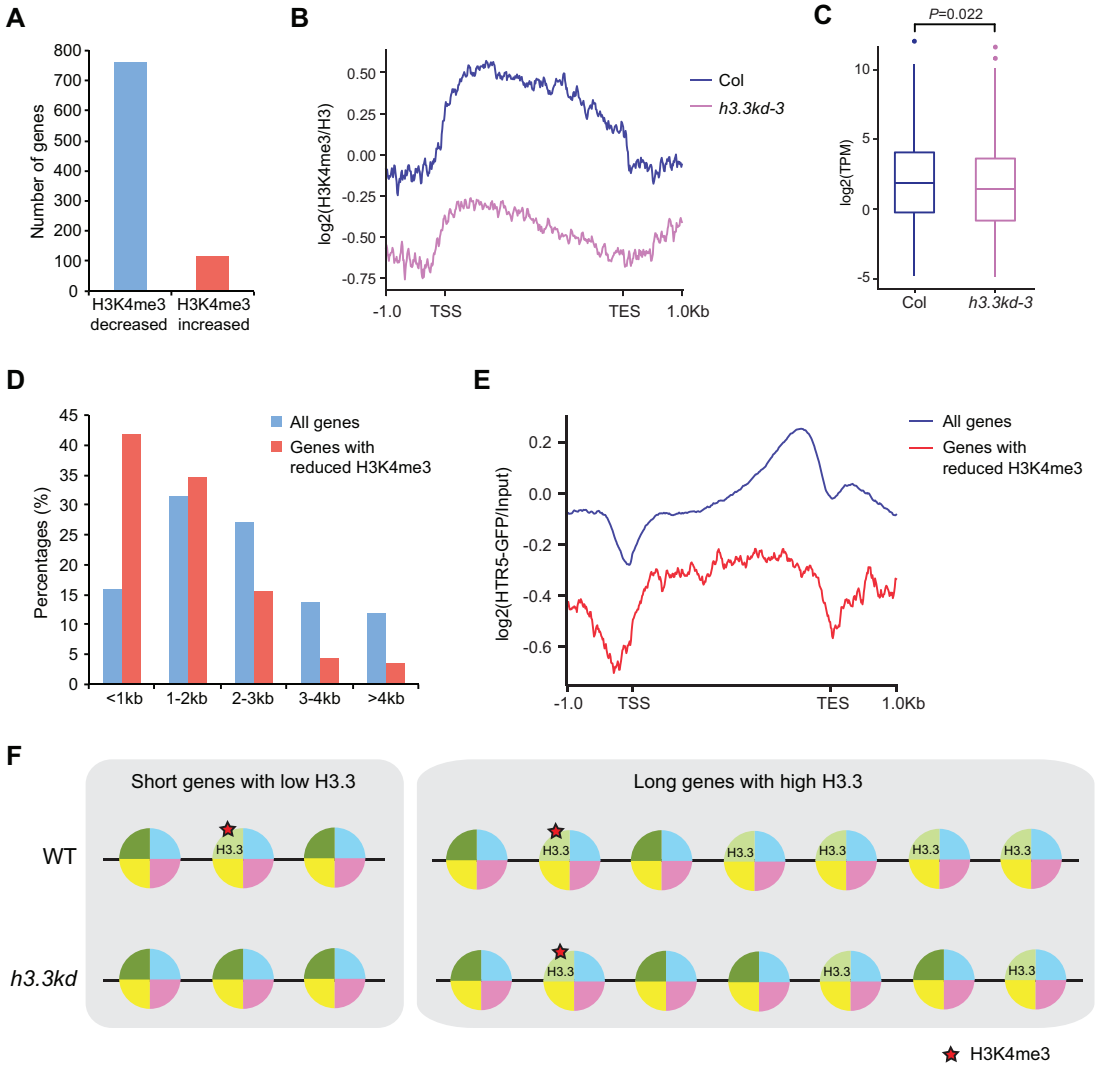

Figure 6 H3K4me3 is reduced at a subset of short genes in *h3.3kd*. A, The number of H3K4me3 decreased and increased genes in *h3.3kd*. B, Normalized ChIP-seq profiles of H3K4me3 enrichment in Col and *h3.3kd-3* over genes with reduced H3K4me3 in *h3.3kd-3*. TSS: transcription start site, TES: transcription end site. C, RNA-seq determined expression profiles of genes with reduced H3K4me3 in *h3.3kd-3*. The *P*-value is based on the Mann–Whitney *U* test. The RNA-seq data were generated in a previous study (Wollmann et al., 2017). D, Gene length distribution of all genes and genes with reduced H3K4me3 in *h3.3kd-3*. E, Normalized ChIP-seq profiles of HTR5-GFP enrichment in Col over all genes and genes with reduced H3K4me3 in *h3.3kd-3*. F, A possible explanation for the predominant loss of H3K4me3 at short genes with low levels of H3.3 in *h3.3kd*. At their loci, limited supply of H3.3 in *h3.3kd* may lead to a near-complete depletion of H3.3, which likely serves as a substrate for H3K4me3 or directly regulates H3K4me3 at nearby nucleosomes, resulting in strong H3K4me3 reduction. At long genes with high levels of H3.3, a considerable amount of H3.3 could be kept at their loci in *h3.3kd*, which is enough to maintain H3K4me3.

enriched with short genes (Figure 6D). H3.3 distribution was further analyzed by profiling chromatin occupancy of HTR5-GFP in seedlings using ChIP-seq. Like H3K4me3, H3.3 tended to occupy the whole body of short genes (Supplemental Figure S5B). Moreover, genes with reduced H3K4me3 in *h3.3kd* had less H3.3 accumulation compared with the average level (Figure 6E), suggesting that the H3K4me3 is more vulnerable at genes where H3.3 could be nearly depleted when a limited amount of it is available in *h3.3kd* (Figure 6F).

Discussion

On the Arabidopsis genome, H3.3 preferentially associates with active genes, but the function of H3.3 on transcription and chromatin regulation is still not clear. The knockdown of H3.3 causes leaf serration, reduced fertility, and misexpression of particularly responsive genes (Wollmann et al., 2017). The early flowering phenotype and reduced expression of *FLC* and its homologs in *h3.3kd* indicate that H3.3 also regulates the floral transition (Figure 1; Supplemental Figure S1). The loss of H3.3 may directly affect transcription as

H3.3-containing nucleosomes are less stable (Jin and Felsenfeld, 2007). However, the majority of the H3.3-enriched genes expressed normally upon H3.3 knockdown, suggesting that the loss of H3.3 itself may not directly or be significant enough to affect transcription (Wollmann et al., 2017). Our results show that H3.3 promotes the deposition of active histone modifications at *FLC*, *MAF4*, and *MAF5* (Figure 2; Supplemental Figure S2). Moreover, H3K4me3 reduction induced by H3.3 knockdown is coupled with reduced gene transcription (Figure 6C). It is possible that decreased active histone modifications, together with the lack of H3.3 deposition, contribute to the reduced expression of *FLC* and its homologs in *h3.3kd*.

In the absence of *FRI*, H3.3 is enriched at both *FLC* 5′ and 3′ ends (Figure 4A). In winter annuals, FRI directly associates with HIRA and stimulates H3.3 deposition at *FLC* gene body and 3′ end (Figure 4, A–D), and elevated H3.3 facilitates FRI-induced 5′ end enrichment of H3K4me3 and H3K36me3 at *FLC* (Figure 3, D and E). We show that H3.3 promotes the *FLC* 5′ to 3′ looping (Figure 4E), which may explain how 3′-enriched H3.3 enhances active histone modifications at the 5′ end. The COMPASS-like complex binds both the *FLC* 5′ and 3′ ends and is required for FRI-induced loop formation. In addition, H3K4me3 at the *FLC* 3′ end is moderately induced by FRI (Li et al., 2018). H3.3 accumulation at the 3′ end may enhance the activity of histone modifiers and/or stabilize their binding at the spatially nearby 5′ and 3′ ends, resulting in increased active histone modifications and gene loop formation (Figure 4F). It has been reported that genes with a loop structure tend to carry H3.3 at both gene ends (Liu et al., 2016), a pattern similar to that at *FLC*. Therefore, it is of great interest to further investigate the general function of H3.3 at genes with a loop structure.

We found that H3.3 knockdown has minimal effects on H3K4me3 levels at long genes, where H3K4me3 is enriched at the 5′ end; while H3.3 is highly accumulated at the 3′ end (Supplemental Figure S5B; Li et al., 2016). In contrast, H3K4me3 is strongly reduced in *h3.3kd* at particularly short genes, at which H3.3 and H3K4me3 share similar distribution patterns and localize across the whole genic region (Figure 6B; Supplemental Figure S5B; Li et al., 2016), suggesting that H3.3 may serve as a substrate for H3K4me3 or directly regulate H3K4me3 at nearby nucleosomes. This is in line with the reduction of H3K4me3 in *h3.3kd* at the 5′ end of *FLC*, a long gene (~6 kb) but accumulates H3.3 around both TSS and TES. We also noted that genes with strong H3K4me3 reductions in *h3.3kd* carry less H3.3 than average (Figure 6E). *h3.3kd* plants show mild developmental defects, whereas *h3.3* knockout lines are not viable, indicating that a substantial amount of H3.3 is still available in *h3.3kd* (Wollmann et al., 2017). It is possible that at genes with little H3.3, the lack of H3.3 supply caused by H3.3 knockdown could lower its levels below a critical threshold essential for the maintenance of H3K4me3, yet genes with high H3.3 levels may still carry enough H3.3 for H3K4me3 deposition (Figure 6F). Further studies using materials with stronger H3.3 impairment would help to provide a more comprehensive view of the function of H3.3 in histone modifications and chromatin regulation in plants.

Our study shows that although H3K36me3 requires H3.3, the deposition of H3.3 at *FLC* is independent of H3K36me3 (Figure 5F). Hence, H3.3 incorporation is likely the prerequisite of H3K36me3. Recent studies in animals have shown that the phosphorylation at Serine31, a specific amino acid on H3.3, directly impacts H3K36me3 and H3K27ac in-cis (Armache et al., 2020; Sitbon et al., 2020). Plant H3.3 proteins contain a specific threonine at residue 31, which might undergo phosphorylation. It is of note that the alanine at position 31 on H3.1 is specifically recognized by ARABIDOPSIS TRITHORAX-RELATED PROTEIN 5 (ATXR5) and ATXR6, two plant-specific methyltransferases preferentially catalyzing H3K27me1 on H3.1 (Jacob et al., 2009, 2014). The A31 residue on plant H3.1 is also required for the H3K27me3 maintenance, mediated specifically by H3.1 (Jiang and Berger, 2017). The distinct amino acids on H3.1 and H3.3 may stimulate or exclude specific enzymes, and thus enable H3.1 and H3.3 to serve as favored substrates for different types of histone modifications. Alternatively, H3.3 may attract specific binding partners and engage the configuration of chromatin structure suitable for active histone modifications.

Nucleosomes containing both H3.3 and H2A.Z are unstable (Jin and Felsenfeld, 2007). At Arabidopsis gene loci, H3.3 overall opposes H2A.Z accumulation especially at the 3′ gene end (Wollmann et al., 2017). Our results confirmed the antagonism between H3.3 and H2A.Z at *FLC* (Figure 5, E and F). H2A.Z is often associated with transcriptional repression, but at the *FLC* locus it activates its expression. Interestingly, it has been reported that the H2A.Z abundance at *FLC* is not positively associated with *FLC* expression levels, rather the less *FLC* is expressed, the higher H2A.Z is enriched (Deal et al., 2007). This is in line with our observations that H3.3 knockdown induces H2A.Z accumulation but leads to decreased *FLC* expression. These results suggest that in Col, the presence of both H3.3 and H2A.Z is required for the *FLC* activation while lacking either one compromises *FLC* expression. Hence, balanced H3.3 and H2A.Z deposition may help to smooth the transcription process and establish a competent state for *FLC* transcription. H3.3 and H2A.Z are both enriched at the *FLC* 5′ and 3′ ends (Figures 4A; 5, E and F). It is tempting to speculate that at *FLC*, H3.3 and H2A.Z co-exist in the same nucleosomes, which are highly sensitive to disruption. In contrast, the loss of either H2A.Z or H3.3 increases the nucleosome stability and transcription blockage at *FLC*, resulting in a less competent state for transcription.

Materials and methods

Plant materials and growth conditions

Arabidopsis (*A. thaliana*) *h3.3kd* lines (Wollmann et al., 2017), *h2a.z* (Coleman-Derr and Zilberman, 2012), *FRI*-Col (Lee et al., 1994), *fve-4* (Kim et al., 2004), *fld-3* (He et al., 2003), *flc-3* (Michaels and Amasino, 1999), *efs-3* (Kim et al.,

2005), and *HTR5-GFP* (Wollmann et al., 2012) were described previously. Since in *h2a.z* (*hta8*; *hta9*; *hta11*), the *hta8* mutant was derived from the Ws (Wassilewskija) background, *h2a.z* was backcrossed with Col three times prior to any analyses. Plants were grown in long days (16 h light/8 h dark) or short days (8 h light/16 h dark) at ~22°C.

RNA analysis

Total RNAs from 10-day-old seedlings were extracted with Minibest plant RNA extraction kit (Takara). Reverse transcription was performed using TransScript one-step gDNA removal and cDNA synthesis supermix (TransGen). RT-qPCR was carried out on an Applied Biosystems QuantStudio 6 Flex Real-Time PCR System using TransStart top green qPCR supermix (TransGen). *TUB2* was used as an endogenous control for normalization. Primers used for amplification are listed in Supplemental Table S2.

For the analysis of published RNA-seq data (Wollmann et al., 2017), reads were mapped to the Arabidopsis genome (TAIR10) using Hisat2 (Kim et al., 2019). Reads per gene were counted by HTseq (Anders et al., 2015), and transcripts per million values were generated using R.

ChIP-qPCR

ChIP experiments were carried out using sonicated chromatin extracted from 10-day-old seedlings as previously described (Jiang and Berger, 2017). Immunoprecipitations were performed with anti-H3 (Abcam, ab1791), anti-H3K4me3 (Abcam, ab8580), anti-H3K36me3 (Abcam, ab9050), anti-H3K27me3 (Millipore, 07-449), and anti-H2A.Z (Yelagandula et al., 2014) antibodies. ChIP with HTR5-GFP-related lines were conducted with GFP-trap agarose beads (Chromotek, gta-20). The amounts of immunoprecipitated DNA were quantified by quantitative real-time PCR (qPCR). Primers used for amplification are specified in Supplemental Table S2.

ChIP-seq analysis

To analyze genome-wide H3K4me3 changes in *h3.3kd*, published ChIP-seq datasets were downloaded (Wollmann et al., 2017), and reads were aligned to the Arabidopsis genome (TAIR10) with Botiew2 (Langmead and Salzberg, 2012). Reads were filtered for duplicated reads by using Picard MarkDuplicates (https://github.com/broadinstitute/picard). For data visualization, bigwig coverage files of H3K4me3 relative to H3 ($\log_2$ ratio) were generated using deepTools utility bamCoverage with a bin size of 10 bp (Ramirez et al., 2014). To identify differential H3K4me3 enriched genes, the average scores for H3K4me3/H3 over the whole gene body were calculated with deepTools utility multiBigwigSummary, genes with H3K4me3/H3 ratio more than one in Col were retained for further analysis and differential genes were called by requiring more than 1.5-fold difference in *h3.3kd* compared with Col. Average ChIP-seq profiles were generated using deepTools utility plotProfile.

To profile HTR5-GFP enrichment in 10-day-old seedlings, materials were ground with liquid nitrogen into fine powder and fixed with 1% (v/v) formaldehyde, followed by nuclei extraction and micrococcal nuclease (Sigma, N5386) digestion to generate mononucleosomes as previously described (Jiang and Berger, 2017). Immunoprecipitation was performed with GFP-trap agarose beads (Chromotek, gta-20). ChIP-recovered DNA was subjected to library preparation with VAHTS universal DNA library prep kit for Illumina (Vazyme, ND607) according to manufacturer's instruction and sequenced with HiSeq 2500 to generate paired-end 150-bp reads. Adapter trimming was performed and low quality reads were filtered with fastp (Chen et al., 2018). Reads were mapped to the Arabidopsis genome (TAIR10) with Botiew2 (Langmead and Salzberg, 2012), and filtered for duplicated reads by using Picard MarkDuplicates (https://github.com/broadinstitute/picard). For data visualization, bigwig coverage files of HTR5-GFP relative to input ($\log_2$ ratio) were generated using deepTools utility bamCoverage with a bin size of 10 bp (Ramirez et al., 2014). Average ChIP-seq profiles were generated using deepTools utility plotProfile.

Pull-down assay

Full-length coding regions of *HIRA* and *FRI* were cloned into pGEX-5X-2 and pRSETA for the production of GST-HIRA and His-FRI proteins respectively. Proteins were expressed using *Escherichia coli* BL21 (DE3) by IPTG induction. GST-HIRA and His-FRI were mixed together with glutathione-agarose resin (GE Healthcare) in pull-down buffer (50-mM Tris pH 7.5, 150-mM NaCl, 1-mM EDTA, 0.5% Nonidet P-40, protease inhibitor cocktail) at 4°C overnight. After washing four times with pull-down buffer, proteins retained on the beads were eluted by boiling with sodium dodecyl sulfate (SDS) loading buffer, separated by SDS–polyacrylamide gel electrophoresis, and detected with anti-GST (Sigma, G7781) and anti-His (CWBio, CW0286) antibodies. Primers used for generating constructs are listed in Supplemental Table S2.

Western blot

To analyze HTR5-GFP expression, total proteins extracted from 10-day-old seedlings were transferred to a 0.2-μm nitrocellulose membrane and detected with anti-GFP (TransGen, HT801) and anti-Actin (CWBio, CW0264) antibodies.

Bimolecular fluorescence complementation

The full-length coding sequences of FRI and HIRA were cloned into pEarleyGate201-YN and pEarleyGate202-YC vectors (Lu et al., 2010) via gateway technology (Thermo Fisher Scientific) and subsequently transformed into *Agrobacterium tumefaciens* strain GV3101. The *Agrobacterium* strains harboring YN, YC, and mRFP-AHL22 were coinfiltrated into *Nicotiana benthamiana* plant leaves. YFP and mRFP signals were observed 2–3 days after infiltration using a Zeiss confocal laser scanning microscope. For detecting YFP signals, excitation was performed at 514 nm (2% laser intensity), and emission was collected at 519–579 nm (gain: 972). For detecting mRFP signals, excitation was performed at 561 nm (2% laser intensity), and emission was collected

at 578–650 nm (gain: 700). Primers used for generating constructs are listed in Supplemental Table S2.

Co-IP assay

To express tag-fused FRI and HIRA, CaMV 35S promoter was first inserted into pGWB513 and pGWB516 (Nakagawa et al., 2007), subsequently the full-length coding sequences of FRI and HIRA except stop codon were inserted to fuse with HA and Myc in pGWB513 and pGWB516 respectively. Protoplast transformation was performed as previously described (Cheng et al., 2015). After transformation, protoplasts were kept overnight and subjected to total protein extraction with Co-IP buffer (50-mM HEPES, pH 7.5, 150-mM KCl, 1-mM EDTA, 1-mM DTT, 0.3% Triton X-100, protease inhibitor cocktail). After centrifugation, the supernatant was incubated with anti-HA beads (Thermo scientific, 88836) for overnight. Tagged proteins were detected with anti-Myc (Easybio, BE2011) and anti-HA (CST, 3724) antibodies. Primers used for generating constructs are listed in Supplemental Table S2.

3C experiment

3C experiment was performed as previously described (Louwers et al., 2009; Crevillen et al., 2013; Li et al., 2018). Briefly, nuclei extracted from freshly collected 10-day-old seedlings were fixed with 2% formaldehyde and subsequently lysed with 0.2% SDS at 65°C for 30 min. SDS was sequestered with 2% Triton X-100 at 37°C for 1 h. *BamH*I and *Bgl*II were used to digest chromatin overnight and were inactivated with 1.6% SDS. After the sequestration of SDS with 1% Triton X-100, ligation was performed at 16°C for 5 h with T4 DNA ligase, followed by reverse crosslink and DNA recovery.

Relative interaction frequencies were quantified and calculated as described previously (Crevillen et al., 2013; Li et al., 2018). Amplifications of a loading control region that does not contain restriction sites were used to normalize DNA concentration between samples. Primer efficiency was normalized by amplification with a control template DNA consists of equal amounts of all possible ligation products, which was generated by ligating a *BamH*I and *Bgl*II cut plasmid containing an 11-kb *FLC* genomic fragment (Li et al., 2018). Values are averages of three biological replicates. Primers used for amplification were adopted from a previous study (Li et al., 2018).

Statistical analysis

Statistical significance was determined with two-tailed Student's *t* test, one-way Analysis of Variance (ANOVA) with Tukey's test or Mann–Whitney *U* test.

Data availability

The published H3K4me3 and RNA-seq datasets were downloaded from GEO GSE96873. The ChIP-seq data of HTR5-GFP in seedlings are available in the GEO under accession number GSE167384.

Accession numbers

FLC (AT5G10140), *FLM/MAF1* (AT1G77080), *MAF2* (AT5G65050), *MAF3* (AT5G65060), *MAF4* (AT5G65070), *MAF5* (AT5G65080), *HIRA* (AT3G44530), *ASF1a* (AT1G66740), *ASF1b* (AT5G38110), *FRI* (AT4G00650), *FVE* (AT2G19520), *FLD* (AT3G10390), *EFS/SDG8* (AT1G77300), *HTR5* (AT4G40040).

Supplemental data

The following materials are available in the online version of this article.

Supplemental Figure S1. Flowering phenotype and gene expression analyses in *h3.3kd* lines.

Supplemental Figure S2. Chromatin modification changes at *MAF4* and *MAF5* in *h3.3kd-1*.

Supplemental Figure S3. *h3.3kd-1* represses the late flowering phenotype of *fve-4* and *fld-3*.

Supplemental Figure S4. HTR5-GFP and *FLC* expression in HTR5-GFP-related lines.

Supplemental Figure S5. ChIP-seq analysis of H3K4me3 and HTR5-GFP distribution.

Supplemental Table S1. List of genes at which H3K4me3 changed more than 1.5-fold in *h3.3kd-3*.

Supplemental Table S2. Primer sequences used in this study.

Acknowledgments

We thank Hui Li and Mande Xue (Institute of Genetics and Developmental Biology, Chinese Academy of Sciences) for their assistance with the experiments.

Funding

This work was supported by the National Key R&D Program of China Grant (grant no. 2019YFA0903903), the Strategic Priority Research Program of the Chinese Academy of Sciences (Precision Seed Design and Breeding, grant no. XDA24020303) and the National Natural Science Foundation of China (grant no. 31970527).

Conflict of interest statement. None declared.

References

Anders S, Pyl PT, Huber W (2015) HTSeq-a Python framework to work with high-throughput sequencing data. Bioinformatics **31**: 166–169

Armache A, Yang S, de Paz AM, Robbins LE, Durmaz C, Cheong JQ, Ravishankar A, Daman AW, Ahimovic DJ, Klevorn T, et al. (2020) Histone H3.3 phosphorylation amplifies stimulation-induced transcription. Nature **583**: 852–857

Ausin I, Alonso-Blanco C, Jarillo JA, Ruiz-Garcia L, Martinez-Zapater JM (2004) Regulation of flowering time by FVE, a retinoblastoma-associated protein. Nat Genet **36**: 162–166

Banaszynski LA, Wen DC, Dewell S, Whitcomb SJ, Lin MY, Diaz N, Elsasser SJ, Chapgier A, Goldberg AD, Canaani E, et al. (2013) Hira-dependent histone H3.3 deposition facilitates PRC2 recruitment at developmental loci in ES cells. Cell **155**: 107–120

Bao S, Hua C, Shen L, Yu H (2020) New insights into gibberellin signaling in regulating flowering in Arabidopsis. J Integr Plant Biol **62**: 118–131

Borg M, Jiang D, Berger F (2021) Histone variants take center stage in shaping the epigenome. Curr Opin Plant Biol **61**: 101991

Chang YN, Zhu C, Jiang J, Zhang H, Zhu JK, Duan CG (2020) Epigenetic regulation in plant abiotic stress responses. J Integr Plant Biol **62**: 563–580

Chen SF, Zhou YQ, Chen YR, Gu J (2018) fastp: an ultra-fast all-in-one FASTQ preprocessor. Bioinformatics **34**: 884–890

Cheng Z, Li JF, Niu Y, Zhang XC, Woody OZ, Xiong Y, Djonovic S, Millet Y, Bush J, McConkey BJ, et al. (2015) Pathogen-secreted proteases activate a novel plant immune pathway. Nature **521**: 213–216

Choi K, Kim J, Hwang HJ, Kim S, Park C, Kim SY, Lee I (2011) The FRIGIDA complex activates transcription of FLC, a strong flowering repressor in Arabidopsis, by recruiting chromatin modification factors. Plant Cell **23**: 289–303

Coleman-Derr D, Zilberman D (2012) Deposition of histone variant H2A.Z within gene bodies regulates responsive genes. PLoS Genet **8**: e1002988

Crevillen P, Sonmez C, Wu Z, Dean C (2013) A gene loop containing the floral repressor FLC is disrupted in the early phase of vernalization. EMBO J **32**: 140–148

Deal RB, Topp CN, McKinney EC, Meagher RB (2007) Repression of flowering in Arabidopsis requires activation of FLOWERING LOCUS C expression by the histone variant H2A.Z. Plant Cell **19**: 74–83

Ding Y, Ndamukong I, Xu ZS, Lapko H, Fromm M, Avramova Z (2012) ATX1-generated H3K4me3 is required for efficient elongation of transcription, not initiation, at ATX1-regulated genes. PloS Genet **8**: e1003111

Duc C, Benoit M, Detourne G, Simon L, Poulet A, Jung M, Veluchamy A, Latrasse D, Le Goff S, Cotterell S, et al. (2017) Arabidopsis ATRX modulates H3.3 occupancy and fine-tunes gene expression. Plant Cell **29**: 1773–1793

Duc C, Benoit M, Le Goff S, Simon L, Poulet A, Cotterell S, Tatout C, Probst AV (2015) The histone chaperone complex HIR maintains nucleosome occupancy and counterbalances impaired histone deposition in CAF-1 complex mutants. Plant J **81**: 707–722

Fan JY, Gordon F, Luger K, Hansen JC, Tremethick DJ (2002) The essential histone variant H2A.Z regulates the equilibrium between different chromatin conformational states. Nat Struct Biol **9**: 172–176

Goldberg AD, Banaszynski LA, Noh KM, Lewis PW, Elsaesser SJ, Stadler S, Dewell S, Law M, Guo X, Li X, et al. (2010) Distinct factors control histone variant H3.3 localization at specific genomic regions. Cell **140**: 678–691

Gu XF, Le C, Wang YZ, Li ZC, Jiang DH, Wang YQ, He YH (2013) Arabidopsis FLC clade members form flowering-repressor complexes coordinating responses to endogenous and environmental cues. Nat Commun **4**:1947

Hake SB, Allis CD (2006) Histone H3 variants and their potential role in indexing mammalian genomes: the "H3 barcode hypothesis. Proc Natl Acad Sci USA **103**: 6428–6435

He Y (2012) Chromatin regulation of flowering. Trends Plant Sci **17:** 556–562

He Y, Michaels SD, Amasino RM (2003) Regulation of flowering time by histone acetylation in Arabidopsis. Science **302**: 1751–1754

Hodl M, Basler K (2009) Transcription in the absence of histone H3.3. Curr Biol **19**: 1221–1226

Jacob Y, Bergamin E, Donoghue MT, Mongeon V, LeBlanc C, Voigt P, Underwood CJ, Brunzelle JS, Michaels SD, Reinberg D, et al. (2014) Selective methylation of histone H3 variant H3.1 regulates heterochromatin replication. Science **343**: 1249–1253

Jacob Y, Feng S, LeBlanc CA, Bernatavichute YV, Stroud H, Cokus S, Johnson LM, Pellegrini M, Jacobsen SE, Michaels SD (2009) ATXR5 and ATXR6 are H3K27 monomethyltransferases required for chromatin structure and gene silencing. Nat Struct Mol Biol **16**: 763–768

Jang CW, Shibata Y, Starmer J, Yee D, Magnuson T (2015) Histone H3.3 maintains genome integrity during mammalian development. Genes Dev **29**: 1377–1392

Jarillo JA, Pineiro M (2015) H2A.Z mediates different aspects of chromatin function and modulates flowering responses in Arabidopsis. Plant J **83**: 96–109

Jiang D, Berger F (2017) DNA replication-coupled histone modification maintains Polycomb gene silencing in plants. Science **357**: 1146–1149

Jiang D, Berger F (2017) Histone variants in plant transcriptional regulation. Biochim Biophys Acta Gene Regul Mech **1860**: 123–130

Jiang D, Gu X, He Y (2009) Establishment of the winter-annual growth habit via FRIGIDA-mediated histone methylation at FLOWERING LOCUS C in Arabidopsis. Plant Cell **21**: 1733–1746

Jiang D, Kong NC, Gu X, Li Z, He Y (2011) Arabidopsis COMPASS-like complexes mediate histone H3 lysine-4 trimethylation to control floral transition and plant development. PLoS Genet **7**: e1001330

Jiang D, Wang Y, Wang Y, He Y (2008) Repression of FLOWERING LOCUS C and FLOWERING LOCUS T by the Arabidopsis Polycomb repressive complex 2 components. PLoS One **3**: e3404

Jiang P, Wang S, Jiang H, Cheng B, Wu K, Ding Y (2018) The COMPASS-like complex promotes flowering and panicle branching in rice. Plant Physiol **176**: 2761–2771

Jin CY, Felsenfeld G (2007) Nucleosome stability mediated by histone variants H3.3 and H2A.Z. Genes Dev **21**: 1519–1529

Johanson U, West J, Lister C, Michaels S, Amasino R, Dean C (2000) Molecular analysis of FRIGIDA, a major determinant of natural variation in Arabidopsis flowering time. Science **290**: 344–347

Kim D, Paggi JM, Park C, Bennett C, Salzberg SL (2019) Graph-based genome alignment and genotyping with HISAT2 and HISAT-genotype. Nat Biotechnol **37**: 907–915

Kim DH, Sung S (2010) The Plant Homeo Domain finger protein, VIN3-LIKE 2, is necessary for photoperiod-mediated epigenetic regulation of the floral repressor, MAF5. Proc Natl Acad Sci USA **107**: 17029–17034

Kim HJ, Hyun Y, Park JY, Park MJ, Park MK, Kim MD, Kim HJ, Lee MH, Moon J, Lee I, et al. (2004) A genetic link between cold responses and flowering time through FVE in Arabidopsis thaliana. Nat Genet **36**: 167–171

Kim SY, He YH, Jacob Y, Noh YS, Michaels S, Amasino R (2005) Establishment of the vernalization-responsive, winter-annual habit in Arabidopsis requires a putative histone H3 methyl transferase. Plant Cell **17**: 3301–3310

Ko JH, Mitina I, Tamada Y, Hyun Y, Choi Y, Amasino RM, Noh B, Noh YS (2010) Growth habit determination by the balance of histone methylation activities in Arabidopsis. EMBO J **29**: 3208–3215

Langmead B, Salzberg SL (2012) Fast gapped-read alignment with Bowtie 2. Nat Methods **9**: 357–359

Lee I, Michaels SD, Masshardt AS, Amasino RM (1994) The late-flowering phenotype of FRIGIDA and mutations in LUMINIDEPENDENS is suppressed in the Landsberg erecta strain of Arabidopsis. Plant J **6**: 903–909

Li Z, Jiang D, Fu X, Luo X, Liu R, He Y (2016) Coupling of histone methylation and RNA processing by the nuclear mRNA cap-binding complex. Nat Plants **2**: 16015

Li Z, Jiang D, He Y (2018) FRIGIDA establishes a local chromosomal environment for FLOWERING LOCUS C mRNA production. Nat Plants **4**: 836–846

Liu B, Liu Y, Wang B, Luo Q, Shi J, Gan J, Shen WH, Yu Y, Dong A (2019) The transcription factor OsSUF4 interacts with SDG725 in promoting H3K36me3 establishment. Nat Commun **10**: 2999

Liu C, Wang C, Wang G, Becker C, Zaidem M, Weigel D (2016) Genome-wide analysis of chromatin packing in Arabidopsis thaliana at single-gene resolution. Genome Res **26**: 1057–1068

Louwers M, Splinter E, van Driel R, de Laat W, Stam M (2009) Studying physical chromatin interactions in plants using Chromosome Conformation Capture (3C). Nat Protocols **4**: 1216–1229

Lu Q, Tang XR, Tian G, Wang F, Liu KD, Nguyen V, Kohalmi SE, Keller WA, Tsang EWT, Harada JJ, et al. (2010) Arabidopsis

homolog of the yeast TREX-2 mRNA export complex: components and anchoring nucleoporin. Plant J **61**: 259–270

Luo X, He Y (2020) Experiencing winter for spring flowering: a molecular epigenetic perspective on vernalization. J Integr Plant Biol **62**: 104–117

Martire S, Gogate AA, Whitmill A, Tafessu A, Nguyen J, Teng YC, Tastemel M, Banaszynski LA (2019) Phosphorylation of histone H3.3 at serine 31 promotes p300 activity and enhancer acetylation. Nat Genet **51:** 941–946

Meng YY, Wang ZY, Wang YQ, Wang CN, Zhu BT, Liu H, Ji WK, Wen JQ, Chu CC, Tadege M, et al. (2019) The MYB activator WHITE PETAL1 associates with MtTT8 and MtWD40-1 to regulate carotenoid-derived flower pigmentation in Medicago truncatula. Plant Cell **31**: 2751–2767

Michaels SD, Amasino RM (1999) FLOWERING LOCUS C encodes a novel MADS domain protein that acts as a repressor of flowering. Plant Cell **11**: 949–956

Michaels SD, He Y, Scortecci KC, Amasino RM (2003) Attenuation of FLOWERING LOCUS C activity as a mechanism for the evolution of summer-annual flowering behavior in Arabidopsis. Proc Natl Acad Sci USA **100**: 10102–10107

Miller T, Krogan NJ, Dover J, Erdjument-Bromage H, Tempst P, Johnston M, Greenblatt JF, Shilatifard A (2001) COMPASS: a complex of proteins associated with a trithorax-related SET domain protein. Proc Natl Acad Sci USA **98**: 12902–12907

Nakagawa T, Suzuki T, Murata S, Nakamura S, Hino T, Maeo K, Tabata R, Kawai T, Tanaka K, Niwa Y, et al. (2007) Improved gateway binary vectors: high-performance vectors for creation of fusion constructs in transgenic analysis of plants. Biosci Biotechnol Biochem **71**: 2095–2100

Nie X, Wang H, Li J, Holec S, Berger F (2014) The HIRA complex that deposits the histone H3.3 is conserved in Arabidopsis and facilitates transcriptional dynamics. Biol Open **3**: 794–802

Noh YS, Amasino RM (2003) PIE1, an ISWI family gene, is required for FLC activation and floral repression in Arabidopsis. Plant Cell **15**: 1671–1682

Raisner RM, Hartley PD, Meneghini MD, Bao MZ, Liu CL, Schreiber SL, Rando OJ, Madhani HD (2005) Histone variant H2A.Z marks the 5 ' ends of both active and inactive genes in euchromatin. Cell **123**: 233–248

Ramirez F, Dundar F, Diehl S, Gruning BA, Manke T (2014) deepTools: a flexible platform for exploring deep-sequencing data. Nucleic Acids Res **42**: W187–W191

Ratcliffe OJ, Kumimoto RW, Wong BJ, Riechmann JL (2003) Analysis of the Arabidopsis MADS AFFECTING FLOWERING gene family: MAF2 prevents vernalization by short periods of cold. Plant Cell **15**: 1159–1169

Sakai A, Schwartz BE, Goldstein S, Ahmad K (2009) Transcriptional and developmental functions of the H3.3 histone variant in Drosophila. Curr Biol **19**: 1816–1820

Sawatsubashi S, Murata T, Lim J, Fujiki R, Ito S, Suzuki E, Tanabe M, Zhao Y, Kimura S, Fujiyama S, et al. (2010) A histone chaperone, DEK, transcriptionally coactivates a nuclear receptor. Genes Dev **24**: 159–170

Scortecci K, Michaels SD, Amasino RM (2003) Genetic interactions between FLM and other flowering-time genes in Arabidopsis thaliana. Plant Mol Biol **52**: 915–922

Sequeira-Mendes J, Araguez I, Peiro R, Mendez-Giraldez R, Zhang X, Jacobsen SE, Bastolla U, Gutierrez C (2014) The functional topography of the Arabidopsis genome is organized in a reduced number of linear motifs of chromatin states. Plant Cell **26**: 2351–2366

Sitbon D, Boyarchuk E, Dingli F, Loew D, Almouzni G (2020) Histone variant H3.3 residue S31 is essential for Xenopus gastrulation regardless of the deposition pathway. Nat Commun **11**: 1256

Smith S, Stillman B (1989) Purification and characterization of CAF-I, a human cell factor required for chromatin assembly during DNA replication in vitro. Cell **58**: 15–25

Stroud H, Otero S, Desvoyes B, Ramirez-Parra E, Jacobsen SE, Gutierrez C (2012) Genome-wide analysis of histone H3.1 and H3.3 variants in Arabidopsis thaliana. Proc Natl Acad Sci USA **109**: 5370–5375

Szenker E, Lacoste N, Almouzni G (2012) A developmental requirement for HIRA-dependent H3.3 deposition revealed at gastrulation in Xenopus. Cell Rep **1**: 730–740

Szenker E, Ray-Gallet D, Almouzni G (2011) The double face of the histone variant H3.3. Cell Res **21**: 421–434

Tagami H, Ray-Gallet D, Almouzni G, Nakatani Y (2004) Histone H3.1 and H3.3 complexes mediate nucleosome assembly pathways dependent or independent of DNA synthesis. Cell **116**: 51–61

Talbert PB, Henikoff S (2017) Histone variants on the move: substrates for chromatin dynamics. Nat Rev Mol Cell Biol **18**: 115–126

Wang H, Jiang D, Axelsson E, Lorkovic ZJ, Montgomery S, Holec S, Pieters B, Al Temimi AHK, Mecinovic J, Berger F (2018) LHP1 interacts with ATRX through plant-specific domains at specific loci targeted by PRC2. Mol Plant **11**: 1038–1052

Wirbelauer C, Bell O, Schubeler D (2005) Variant histone H3.3 is deposited at sites of nucleosomal displacement throughout transcribed genes while active histone modifications show a promoter-proximal bias. Genes Dev **19**: 1761–1766

Wollmann H, Holec S, Alden K, Clarke ND, Jacques PE, Berger F (2012) Dynamic deposition of histone variant H3.3 accompanies developmental remodeling of the Arabidopsis transcriptome. PLoS Genet **8**: e1002658

Wollmann H, Stroud H, Yelagandula R, Tarutani Y, Jiang D, Jing L, Jamge B, Takeuchi H, Holec S, Nie X, et al. (2017) The histone H3 variant H3.3 regulates gene body DNA methylation in Arabidopsis thaliana. Genome Biol **18**: 94

Xu D, Liu Q, Chen G, Yan Z, Hu H (2020) Aldehyde dehydrogenase ALDH3F1 involvement in flowering time regulation through histone acetylation modulation on FLOWERING LOCUS C. J Integr Plant Biol **62**: 1080–1092

Xu L, Zhao Z, Dong A, Soubigou-Taconnat L, Renou JP, Steinmetz A, Shen WH (2008) Di- and tri- but not monomethylation on histone H3 lysine 36 marks active transcription of genes involved in flowering time regulation and other processes in Arabidopsis thaliana. Mol Cell Biol **28**: 1348–1360

Yang H, Howard M, Dean C (2014) Antagonistic roles for H3K36me3 and H3K27me3 in the cold-induced epigenetic switch at Arabidopsis FLC. Curr Biol **24**: 1793–1797

Yelagandula R, Stroud H, Holec S, Zhou K, Feng S, Zhong X, Muthurajan UM, Nie X, Kawashima T, Groth M, et al. (2014) The histone variant H2A.W defines heterochromatin and promotes chromatin condensation in Arabidopsis. Cell **158**: 98–109

Zhou JX, Liu ZW, Li YQ, Li L, Wang B, Chen S, He XJ (2018) Arabidopsis PWWP domain proteins mediate H3K27 trimethylation on FLC and regulate flowering time. J Integr Plant Biol **60**: 362–368

Zhu Y, Weng MJ, Yang Y, Zhang C, Li Z, Shen WH, Dong AW (2011) Arabidopsis homologues of the histone chaperone ASF1 are crucial for chromatin replication and cell proliferation in plant development. Plant J **66**: 443–455